A. Risitano et alii, Frattura ed Integrità Strutturale, 30 (2014) 201-210; DOI: 10.3221/IGF-ESIS.30.26

Focussed on: Fracture and Structural Integrity related Issues

Definition of the linearity loss of the surface temperature in static tensile tests

A. Risitano, G. Fargione
University of Catania, Department of Industrial Engineering, Viale Andrea Doria, 6 - 95125 Catania (Italy)
arisitan@diim.unict.it, gfargion@diim.unict.it

E. Guglielmino
Università degli Studi di Messina, Dipartimento di Ingegneria Elettronica, Chimica e Ingegneria, Industriale, Contrada Di Dio (S. Agata), 98166 Messina, (Italy), eguglie@unime.it

ABSTRACT. Static tensile tests on material for mechanical constructions have pointed out the linearity loss of the surface temperature with the application of load. This phenomenon is due to the heat generation caused by the local microplasticizations which carry the material to deviate from its completely thermoelastic behavior. The identification of the static load which determines the loss of linearity of the temperature under stress, becomes extremely important to define a first dynamic characterization of the material.
The temperature variations that can be recorded during the static test are often very limited (a few tenths of degree for every 100 MPa in steels) and they require the use of special sensors able to measure very low temperature variations. The experience acquired in such analysis highlighted that, dealing with highly accurate sensors or with particular materials, the identification of the first linearity loss (often by eye) in the temperature curves, can be influenced by the sensibility of the investigator himself and can lead to incorrect estimates. The aim of this work is to validate the above mentioned observations on different steels, by applying the autocorrelation function to the data collected during the application of a static load. This, in order to make the results of the thermal analysis free from the sensitivity of the operator and to make the results as objective as possible, for defining the closest time of the linearity loss in the temperature-time function.

KEYWORDS. Termoelasticity; Fatigue; Autocorrelation function.

INTRODUCTION AND AIM OF THE WORK

The research of more simple and faster methodologies for the determination of the fatigue limit or, generally, the data characterizing the dynamic behavior of the materials, has been the subject of continued interest [1-10]. From more than 30 years, the authors work on the methodologies based on the energy factors such as the heat development during the fatigue tests (Risitano method) [11-15] in order to define the fatigue curves in a very short time compared to the traditional method (stair case); the results of this method (Risitano method) have been then studied and

analyzed by many other researchers [16-28] and now this method is quite normal in use. The analysis of the phenomenon of the heat development has highlighted that the material which is subjected to a dynamic stress higher than its fatigue limit, shows the irreversible phenomena already during the first cycle of application of the fatigue loads. For this reason, the authors checked the first loading ramp for the detection of the first micro heat source, index of irreversible deformed states. Thus, it seemed almost natural to think about the application of all methods able to capture this phenomena during the static test, and in particular to rely on infrared thermal sensors for the surface temperature survey. Since the first analyses of this type which date back to 1987, it has been noted that, using this approach, it was possible to determine the region (stress-strain) in which the material follows the laws of the Thermoelasticity [38, 39]. The Thermal analysis applied to various steels during the static tensile test [29-34], showed that it was possible to define the "fatigue limit" by analyzing the temperature of the hottest point of the specimen surface and determining the point where the slope changes, in the temperature vs. stress curve. On the basis of the first results, other researchers [35, 36] tested the procedure on other materials, different from the steels (composite materials). Until now, the point in which the slope changes was determined by plotting, in the stress-temperature diagram, the first part with a constant slope (part perfectly thermoelastic) and identifying the point where the curve deviates from the linear behavior. This work has a double aim: it wants to confirm the procedure to detect the fatigue limit on different steels and it intends to make the measurement independent by the experience of those who adopt this kind of analysis. It is thought that an analysis of the physical phenomenon could be more appropriate than the analytical study of the function. Therefore, it has been proposed the application of the correlation function to the temperature-time data detected during the static tensile tests. In order to define a future test protocol, the authors would try to define a process methodology based on a method independent from the performer of the tests.

This work describes how to use the correlation function for the surface temperature data, collected during a simple static uniaxial tensile test, we can define the point at which the slope of the stress-temperature curve, changes and, therefore, can be estimated the value of the fatigue limit. It has been verified, in fact, that the value of the load, which influences the loss of linearity in the temperature-load (stress) function, corresponds to zero of the autocorrelation function relative to the values that have been detected by the sensors used for the test

SURFACE TEMPERATURE DURING A STATIC TENSILE TEST

Fig. 1 shows the qualitative trend of the result (σ–ε) of a static monoaxial tensile test for a steel plate specimen. The same diagram shows the evolution of the surface temperature measured on the specimen during the test. In the diagram, P indicates where the temperature trend is not linear. At this point, the stress value is completely different from the limit yield strength and the corresponding deformation will be zero if the sample is unloaded. The analysis of the surface temperature curve while varying the load (in red in the diagram) is perfectly linear up to point P then the slope changes when it is still far from the classic value of yield stress. From that point onwards, the slope of the curve varies continuously until the failure of the specimen.

Analyzing the specimen from a physical point of view, during a static tensile test at a constant load speed [N/s], it is possible to characterize the behavior of the first phase as due to the perfectly elastic relation between the change of temperature ΔT and the stresses (Lord Kelvin' law):

$$\Delta T = -K_m T\, \sigma_m \tag{1}$$

where T is the absolute temperature, K_m is the thermoelastic constant of the material (for steels $3.3 \cdot 10^{-12}$ [Pa^{-1}]) σ_m is the average stress applied to the specimen [39].

After this first phase, starting at the point P (second phase) until the break of the specimen, the change of slope is due to the heat developed for the irreversible deformations, which affect more and more volume of the sample until its failure

For this area (starting from point P) the following law can be applied [31]:

$$T = -K_m T_a \sigma_r \frac{t}{t_r} + \frac{\beta m \sigma_0 \varepsilon_p \left(\frac{t}{t_r}\right)^2}{\rho \sigma_E} + \frac{K_m T_a \sigma_r \left(\frac{t}{t_r}\right)^3}{3} \tag{2}$$

where:

– dV_p is the rate at which the volume V is plastically deformed ($dV_p = V - V_e$);

- S is the original cross-sectional area of the specimen ($S=a\cdot b$);
- a is the specimen width;
- b is the specimen thickness;
- S_l is the lateral parallepiped surface ($S\cong 2V/b$ for $a >> b$);
- l_0 is the original length of the specimen;
- Δl_p is the plastic elongation;
- ε_p is the plastic strain ($\varepsilon_p = \Delta l_p/l_0$);
- k_c is the thermal convection coefficient;
- dT_e is the temperature increment of the elastic crystal as it encounters the ambient temperature;
- dT is the temperature increment of the volume V as it encounters the ambient temperature;
- m is the conversion coefficient; and,
- ρ_1 is the density after deformation.

$$\varepsilon = \varepsilon_0 + t\frac{\varepsilon_0}{t_0} \tag{3}$$

$$\varepsilon_p = \frac{\Delta l_p}{l_0} = v_c\frac{t_r}{t_0} \tag{4}$$

$$v_c = \sigma_r\frac{S}{t_r} \tag{5}$$

where, σ_r is the fracture stress of the specimen and t_r is the time in which the plasticization phenomenon starts. In accordance with the laws of the fracture mechanics, it has been supposed the following law for the plasticization volume:

$$V_p = t^2\frac{V}{t_r^2} \tag{6}$$

$$V_\theta = V - t^2\frac{V}{t_r^2} \tag{7}$$

The transition point between the two phases is where the microscopic deformative irreversible phenomena start and they can be appreciated just referring to non-conventional parameters. The experience gained during the fatigue tests with the evaluation of the damage parameters based on the energy methods, shows that the fatigue rupture occurs (even at a very high number of cycles) when, at a microscopic level, irreversible deformations due to the presence of external or internal defects (inclusions, dislocations, etc.) appear. These deformations, by applying cyclic loads, cause micro-cracks that increase in size (with heat development) until to the complete rupture of the material. The static tensile test, assumed as the first loading ramp of a tensile fatigue stress, can give information about the beginning of the internal heat generated by the local irreversible plastic deformations. If repetitive loads (fatigue load) are applied to the specimen with the macroscopic maximum value of stress equal to that of the first plasticization, the specimen, after a certain number of cycles (high or very high), will break. Based on these considerations and using not conventional and more general definition, for Risitano A. the fatigue limit at high (or very high) number of cycles, is the macroscopic stress for which in a well-defined point (crystal) of the material (even at the microscopic level), microplasticizzations appear . For stress value above this (σ_0 in Fig. 1) and for different values of load ratio R, the specimen will break at different Nr cycles (Fig. 2). And more, for stress value σ less than σ_0 failures will never happen; on the contrary, for σ over σ_0, failures will always occur. We can assume the cycles number Nr for R= -1, as the limit number $Nr_{(lim)}$ (equivalent to the conventional value $2\cdot10^6$) and consequently at this $Nr_{(lim)}$ number, the failures, for different loads ratio R, will occur but only for stress values over the fatigue limit (before defined). Starting from the above mentioned observations, it is possible to define the beginning of the local plasticization phenomena as the stress range for which the fatigue failure can appear. For this purpose, the authors have for a long time identified the external temperature (on the surface of the specimen) as a significant parameter (also because it is more easily detectable) able to provide indications on the deformation state (even microscopic) of stressed material.

MEASUREMENT OF THE TEMPERATURE DURING A TENSILE TEST AND AUTOCORRELATION FUNCTION

As it is well known, the autocorrelaction function is widely used in the Signal Theory [40]. It provides a measurement of how a signal auto correlates itself, it means how much it has in common with itself delayed by a time. It also provides the desired signal cleaned from the noise. Finally, it contains the information about the variations on the time axis. For temperature data recorded during static tensile test, the autocorrelation function has been applied, to make free from the subjective effect, the identification of the point where the temperature-strain function (of the hottest point on the specimen surface), loses the perfectly linear trend, i.e the totally elastic behavior.
The analysis of the static tests carried out on the specimen in order to determine the start of the thermal increment, requires the continuous monitoring during the test of three parameters: applied load, surface temperature and time. Practically, the test machine is set on a constant load speed (N/s) and the temperature on the entire surface of the specimen is detected . Once the thermal images are acquired, the analysis is performed starting from the last images and going back by detecting the temperature of the specimen surface at the points of interest. With this approach, the temperature-time (strain) function of the chose point can be built. The analysis of this function, in accordance with the laws of thermoelasticity, points out that, from a given point, the temperature function loses its linearity, in other words the derivative function for two successive points T(t) e T(t+τ) is not constant but it varies with a certain continuity. Since the collected temperature data are real, in order to locate the first point to this variation and make free the reading from the sensitivity of the operator, it is thought to refer to the autocorrelation function. This choice, based on the physical data, does not introduce factors that can have influence on the value to define . In certain cases, in fact, considering the the sensors accuracy and the presence of background noises, an estimation by tracing the straight line which fits the part perfectly elastic and taking the point P at which the temperature-time function leaves the linear behavior, can lead to values with errors of subjectivity which do not affect the validity of the methodology, strictly linked to the physical phenomenon, but can make the procedure less effective. For the use of the autocorrelation function, it is necessary to record a number of acquisitions of the temperature in the first part of the curve (up to the classic limit yield point) sufficiently high. The commercial systems allow the acquisition of 30 frames per second, enough for this kind of analysis. In this work it was adopted 1 frame/s

STATIC TESTS ANALYSIS

Static mono-axial tensile tests were performed on AISI 1045 (C45) specimens, for which the Tab. 1 reports the chemical composition and the Tab. 2 the physical and mechanical properties. The shape and the dimensions of the specimens are those shown in Fig. 3 and Fig. 4. In particular, were performed two (2) test for each specimen type (notched and not). All static tests were carried out with the testing machine INSTRONG 8501 of 100 kN.

	C	Si	Mn	P	S	Cr	Ni	Mo
%	0.43-0.50	0.40	0.60-0.90	0.035	0.035	0.40	0.40	0.10

Table 1: Chemical composition.

During the whole test, the surface temperature of the specimens has been detected by the Thermo camera FLIR SC7000 LWIR. The data acquisition and the analysis of the (acquired) images have been made with the ALTAIR software. The tests have been always performed with a slew rate imposed and constant equal to 115 N/s. The surface temperature, relative to applied loads, was continually recorded. The number of the images acquired per second was equal to 1. They have allowed to build diagrams like those of Fig. from 5 to 10 where on the x axis is reported the time while on the y axis is reported the applied load (in light blue) and the temperature of the chosen surface point (in yellow). Since the aim of the work was also the validation of the analysis capacity through the use of the autocorrelation function, in order to avoid the edge effects on the temperature values , for the three types of specimens (smooth and notched), the temperature values were measured at the centre of the specimen (see Fig. 11). The collected data are those reported in the above mentioned diagrams (Fig. from 5 to 10).

Density	g/cm³	7.87
Brinell Hardness		163
Ultimate Stress	[MPa]	810
Yield Stress	[MPa]	725
Young Modulus	[GPa]	210
Poisson Modulus		0.29
Ultimate Elongation	%	16
Resilience (Izod)	[J]	30
Thermal Conductivity	[W/m*K]	51.9
Specific Heat	[J/g*K]	0.502
Coefficient of linear expansion	[1E-06/K]	15.1
Electrical Resistivity	[Ohm*cm]	1.42E-05

Table 2: Physical and mechanical properties.

Sorge Specimens	Autocorrelation	"eye estimated"
AISI 1045-P1 SMOOTH (12.5x5)	164.5	172.0
AISI 1045-P2 SMOOTH (12.5x5)	168.9	170.0
AISI 1045-P3 NOTCHED (10.9x5)	183.2	175.0
AISI 1045-P4 NOTCHED (10.9x5)	275.1	225.0
AISI 1045-P5 NOTCHED (8.3x5)	264.7	250.0
AISI 1045-P6 NOTCHED (8.3x5)	212.6	195.0

Table 3: Values of the detected stresses referred to the 6 (P1-P6) specimens.

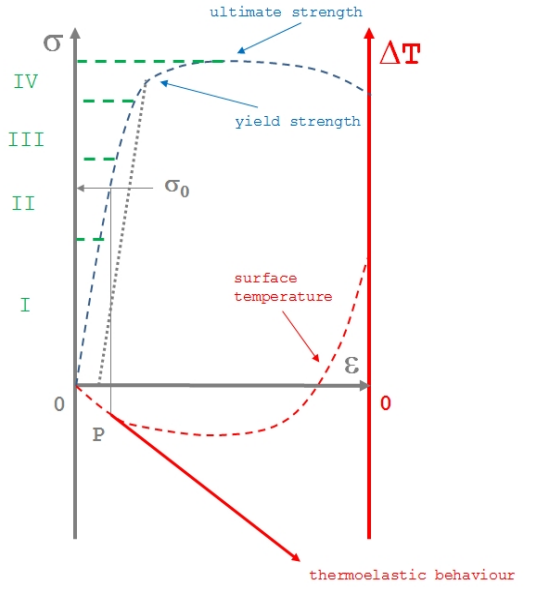

Figure 1: Qualitative stress-strain (σ–ε) curve and Temperature-strain (ΔT-ε) curve of a static monoaxial traction test (indication of σ_0).

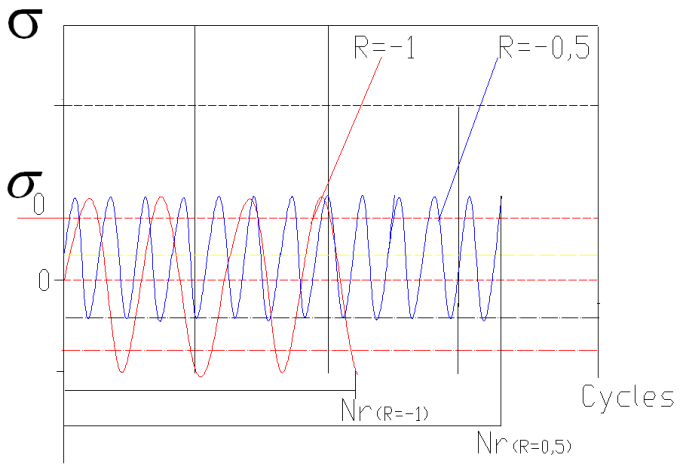

Figure 2: Qualitative failure number cycles for different ratio load but equal σ_{max} ($\sigma_{max} > \sigma_0$).

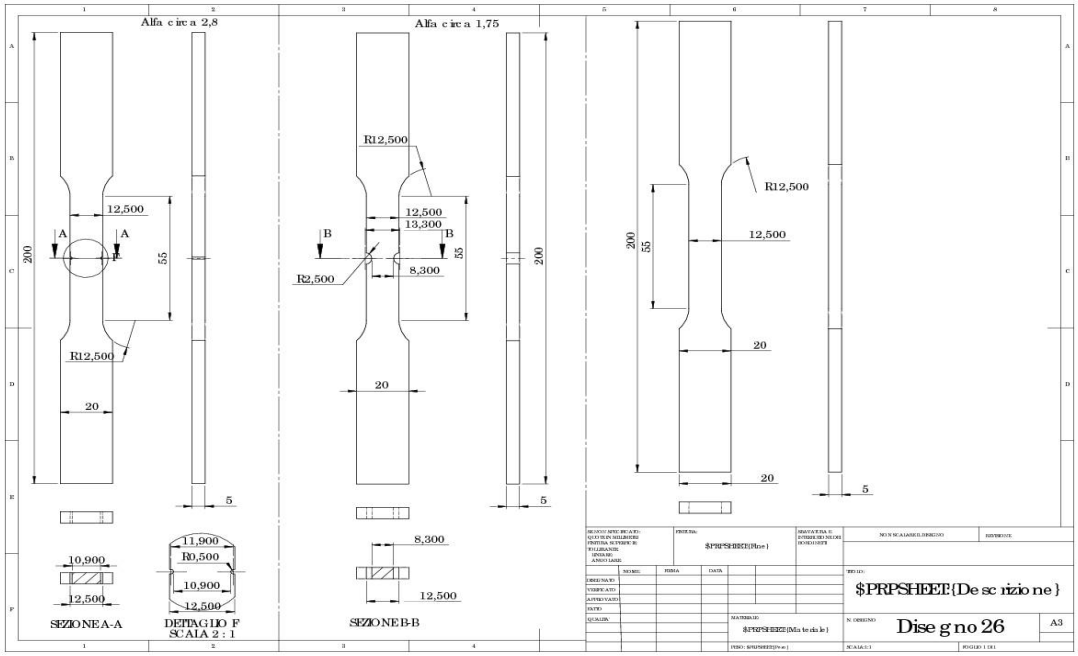

Figure 3: Shape and the dimensions of the specimens.

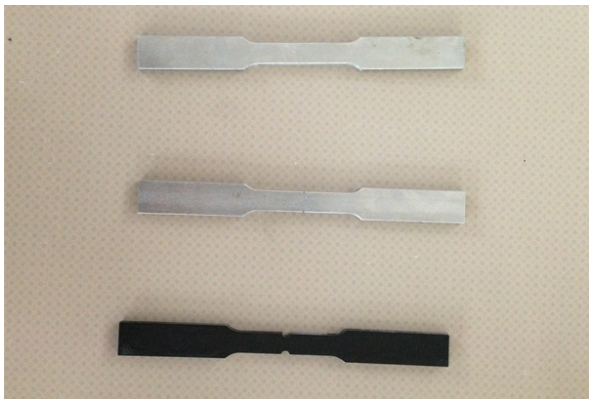

Figure 4: Photos of the three types of specimens (smooth, notched).

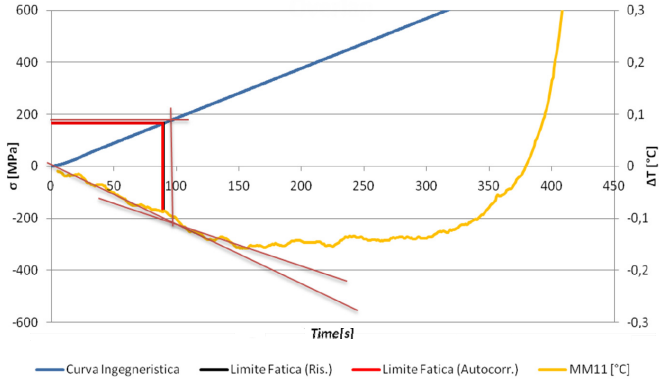

Figure 5: Stress-Time (σ–t) curve and Temperature-Time (ΔT–t) curve for AISI 1045-P1 SMOOTH (12.5x5).

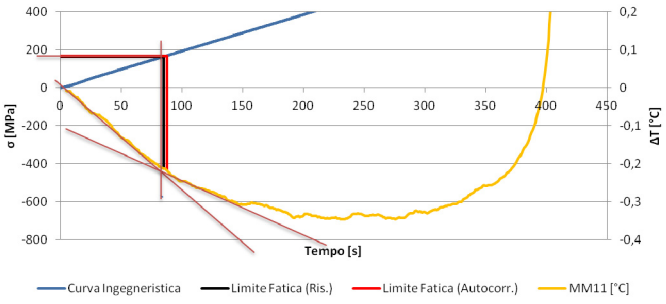

Figure 6: Stress-Time (σ–t) curve and Temperature-Time (ΔT–t) curve for AISI 1045-P1 SMOOTH (12.5x5).

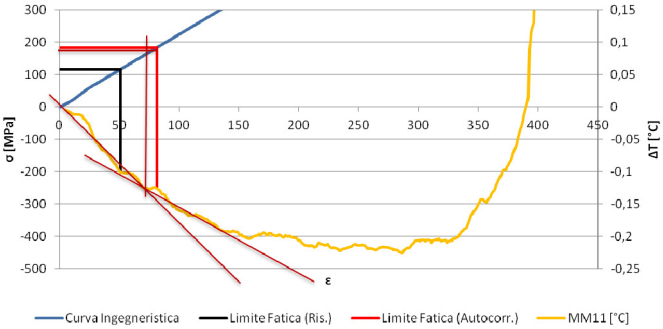

Figure 7: Stress-Time (σ–t) curve and Temperature-Time (ΔT–t) curve for AISI 1045-P3 NOTCHED (10.9x5).

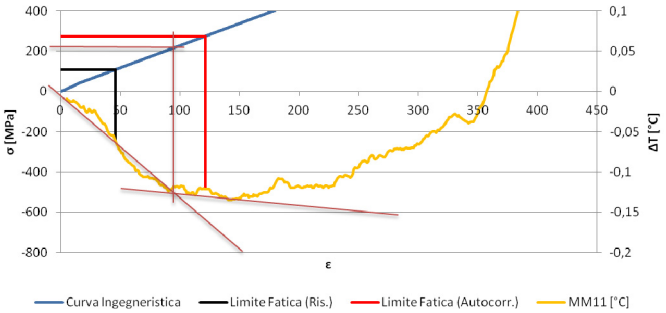

Figure 8: Stress-Time (σ–t) curve and Temperature-Time (ΔT–t) curve for AISI 1045-P4 NOTCHED (10.9x5).

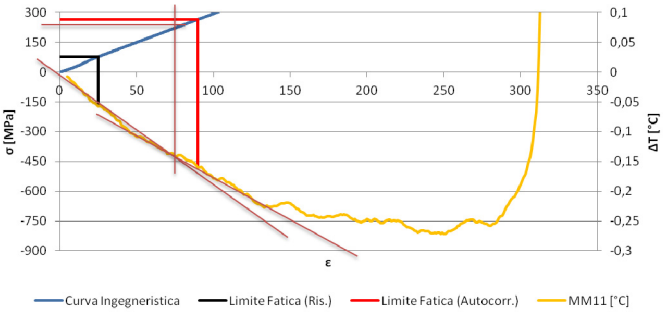

Figure 9: Stress-Time (σ–t) curve and Temperature-Time (ΔT–t) curve for AISI 1045-P5 NOTCHED (8.3x5).

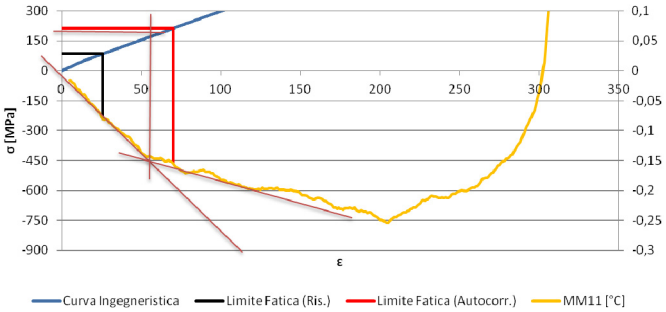

Figure 10: Stress-Time (σ–t) curve and Temperature-Time (ΔT–t) curve for AISI 1045-P6 NOTCHED (8.3x5).

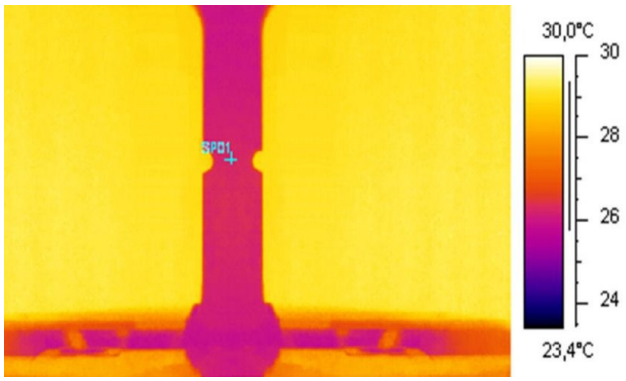

Figure 11: Spot position.

Figures from 5 to 10 report the results of the static tests. In each test is shown the applied load and the temperature detected at the centre of the specimen as a function of the time. In each figure, in correspondence of the time for which the autocorrelation function was zero, it is shown (in red) the vertical line which allowed to date back to the corresponding stress at the point defined by the autocorrelation function. In the diagrams, were reported the lines "by eye" for identification of the change of slope of the temperature and at the intersection of them, it has been identified the corresponding value of the stress (estimated). As before said, the values of the detected stresses, referred to the 6 specimens, are reported in Tab. 3. In this table the first column characterizes the type of specimen, the second column shows the value of the stress estimated "by eye" (eye estimated), the third column shows the values determined by means of the autocorrelation function. The examination of the results of the two columns shows the applicability of the correlation function to the measured temperature data. The differences of the stress values are, in fact, always limited and just in a case there was difference more than 15%. The values determined for the smooth specimens are very close to each other and they are close to those estimated "by eye". The mean value (166.5 N/mm²) for which changes the slope of the curve is very close to the fatigue limit ([171 N/mm²) found for the same steel by the thermographic fatigue method (Risitano method) . It is in the range (170-190 N/mm²), found in literature [41, 42], for a AISI 1045 steel with similar mechanical characteristics and determined by traditional test. As before said, for the notched specimen the analysis was carried out in correspondence to the central point and for this reason the values reported in the table do not represent the fatigue limit, as it was for the smooth specimens, but they are the values and trends depending on the local stresses which, as it is known, during the elastic phase, are less than the mean stress. An analysis carried out close to the edges would determine a different value (lower) of the load for which the change of slope there would be, as it has already reported in [44]. Even for the notched specimens, it has been noticed a good correspondence between the values estimated "by eye" and those found using the autocorrelation function.

CONCLUSIONS

In order to determining the "fatigue limit" (minimum), it has been proposed the use of the autocorrelation function to evaluate the point of the linearity loss of the temperature-time function of a surface point of the specimen during the application of the load in tensile tests. Smooth specimens and notched specimens (2 different notch) were tested. For homogeneity, for each kind of specimen, the analysis has been referred to the central point of the specimen. For each specimen the value of the change of slope of the temperature function over the time (load), corresponding to the end of perfectly and totally elastic behavior, has been identified (by the graphs) with an estimation by eye and by the analysis of the data temperature by means of the autocorrelation function. The results have pointed out the validity of the application of the autocorrelation function to the temperature data. It allows ,in fact, to make the results free from the sensitivity of the operator (estimation by eye). For all the examined cases, the values estimated from the graphs and defined by the autocorrelation function were very close. The obtained results confirm what it has already verified by other authors and also for materials different from the steels. It has confirmed, once again, that the thermal analysis of data collected during the simple static tests allows to estimate with a good approximation the "fatigue limit" of the material. For the AISI 1045 steel the value defined by the tensile test coincides with the value found by other authors [41, 42] who have applied the traditional fatigue tests [43] to the AISI 1045 steel having mechanical properties very similar to the steel used in the present work.

REFERENCES

[1] Locati, L., An aid for the determination of fatigue limit in research and production, Metall. Ital., 27 (1935) 188-204.
[2] Locati, L,. Fatigue and other tests with progressively increasing load, Eng. Dig., 20 (1959) 337-339.
[3] Foppel, O., DieDämpfungsfägsfähikeiteinesBaustahlesbeiWechselbeanspruchungen.V.D.I.Z., 70(39) (1926) 1291-1296.
[4] Prot, M., The determination of the fatigue limit by progressively increased loading, Misure et Control, 13 (1948) 301-309.
[5] Prot, M., Fatigue testing under progressive loading.WADCTR, (1952) 53-148.
[6] Föppl, O., Ludwik, P., StoffprüngegezueinerWirklichkeitsgetreuenFestgkeitsrechnung.V.D.I.Z., 76 (1932) 683-685.
[7] Delorme, J. F., Sinicki, G., Gobin, P., Calorimetric study of the energy dissipated from a solid subjected to fatigue cycles, J. Phys. D: Appl. Phys., 1 (1968) 1737-1742.

[8] Dengel, D., Harig, H., Estimation of the fatigue limit by progressively-increasing load tests, Fatigue Fract. Eng. M.,3 (1980) 113–128.
[9] Kaleta, J., Blotny, R., Harig, H., Energy stored in a specimen under fatigue limit loading conditions, J. Test Eval., 19 (1990) 326–333.
[10] Catalbiano, T., Geraci, A., Orlando M., Analysis of the fatigue strength of specimens by means of the infrared technique, Il Progettista Industriale, 2 (1984).
[11] Geraci, A., La Rosa, G., Risitano, A., L'infrarosso termico nelle applicazioni meccaniche, ATA Ingegneria Automotoristica, 38 (1985) 8-9.
[12] Curti, G., La Rosa, G., Orlando, M., Risitano, A., Analisi tramite infrarosso termico della "temperatura limite" in prove di fatica, In: Proceedings XIV Convegno Nazionale AIAS, (1986) 211-220.
[13] Curti, G., Geraci, A., Risitano, A.. Un nuovo metodo per la determinazione rapida del limite di fatica.ATA IngegneriaAutomotoristica, 10 (1989) 634-636.
[14] La Rosa, G., Risitano, A., Thermographic methodology for rapid determination of the fatigue limit of materials and mechanical components, Int. J. Fatigue, 22 (2000) 65–73.
[15] Fargione, G., Geraci, A., La Rosa, G., Risitano, A., Rapid determination of the fatigue curve by the thermographic method, Int. J. Fatigue, 24 (2002) 11–19.
[16] Luong, M. P., Fatigue limit evaluation of metals using an infrared thermographic technique, Mech. Mater., 28 (1988) 155–163.
[17] Luong, M. P., Infrared thermography of fatigue in metals, SPIE, 1682 (1988) 222-223.
[18] Luong, M. P., Dang-Van, K., Metal fatigue limit using infrared thermography, In: Proceedings Fondazione G. Ronchi, IL (1993).
[19] Luong, M. P., Infrared scanning of fatigue in metals, Nucl. Eng. Des., 158 (1995) 363–376.
[20] Blarasin, A., Fracchia, R., Pozzati, M., Rapid determination of the fatigue limit of materials and components by means of the infrared technique, ATA – Ingegneria Automotoristica, 51 (1988) 255–265.
[21] Curà, F., Curti, G., Sesana, R., A new iteration method for the thermographic determination of fatigue limit in steels, Int. J. Fatigue, 27 (2005) 453–459.
[22] Amiri, M., Khonsari, M.M., Rapid determination of fatigue failure based on temperature evolution: Fully reversed bending load, Int. J. Fatigue, 32 (2010) 382-389.
[23] Liakat, M., Khonsari, M. M., Rapid estimation of fatigue entropy and toughness in metals, Materials and Design, 62 (2014) 149-157
[24] Fatemi, A., Yang, L., Cumulative fatigue damage and life prection theories: a survey of the state of the for homogeneus materials, Int. J. Fatigue, 20 (1998) 9-34.
[25] Feltner, C. E., Morrow, J. D., Microplastic strain hysteresis energy as a criterion for fatigue fracture, J. Basic. Eng., 83 (1961) 15–22.
[26] Walter, F., Eifler, D., Short-time procedure for the determination of Wöehler and fatigue life curves using mechanical, thermal and electrical data, JSMME, 2 (2008) 507-518.
[27] Atzori, B., Meneghetti, G., Energy dissipation in low cycle fatigue of austempered ductile irons, In: Proceedings 5th international conference on low cycle fatigue, (2003) 147–152.
[28] Meneghetti, G., Analysis of the fatigue strength of a stainless steel based on the energy dissipation, Int. J. Fatigue, 29 (2007) 81-94.
[29] Geraci, A., La Rosa, G., Risitano, A., Correlation between thermal variation in static test and elastic limit of material using infrared imagery, In: Proceedings 7th International conference on mechanical behaviour of material (1995).
[30] Risitano, A., Risitano, G., Clienti, C., Determination of fatigue limit by mono-axial tensile specimens using thermal analysis, Key Engineering Materials, 452-453 (2011) 361-364.
[31] Risitano, A., Risitano, G., Determining fatigue limits with thermal analysis of static traction tests, Fatigue Fract. Eng. M., 36 (2013) 631-639.
[32] Risitano, A., Mechanical Design, first ed., CRC Press, New York (2011).
[33] Clienti, C., Fargione, G., La Rosa, G., Risitano, A., Risitano, G., Eng. Fract. Mech., 77 (2010) 2158-2167.
[34] Risitano, A., Corallo, D., Risitano, G., Sirugo, A., Determinazione del limite di fatica mediante prove quasi-statiche, In: Proceedings XXXIX Convegno Nazionale AIAS, (2010).
[35] Bagheri, Z., El Sawi, I., Bougherara, H., Zdero, R., Biomechanical fatigue analysis of an advanced new carbon fiber/flax/epoxy plate for bone fracture repair using conventional fatigue tests and thermography, J. of the Mechanical Behavior of Biomedical Materials, 35 (2014) 27-38.

[36] Colombo, C., Vergani, L., Burman, M., Static and fatigue characterisation of new basalt fibre reinforced composites, Compos. Struct., 94 (2012) 1165-1174.
[37] Libonati, F., Vergani, L., Damage assessment of composite materials by means of thermographic analyses, Compos. Part. B-Eng., 50 (2013) 82-90.
[38] Houwink, R., Burgers, W. G., Elasticity, Plasticity and Structure of Matter, University Press, Cambrige (1954).
[39] Nowacki, W., Thermoelasticity. Pergamon Press, Oxford (1986).
[40] Luise, M., Vitetta, G. M., Teoria dei Segnali, McGraw Hill (2002).
[41] Su, Y.L., Yao, S.H.,Wei, C.S., Kao, W.H., Wu, C.T., Influence of single- and multilayer TiN films on the axial tension and fatigue performance of AISI 1045 steel, Thin Solid Films, 338 (1999) 177–184.
[42] Di Schino, A., Kenny J. M., Grain size dependence of the fatigue behaviour of a ultrafine-grained AISI 304 stainless steel, Mater. Lett., 57 (2003) 3182–3185
[43] ASTM E 466-72, Standard practice for conducting constant amplitude axial test of metallic materials.
[44] Risitano, A., Fargione G., Experimental method for the determination of the under-stress first-plasticization process parameters, In: Proceedings IGF XXII, Rome (Italy), (2013).